

Magnetic Domain Walls in Nanowires

Rolf Allenspach and Pierre-Olivier Jubert

Abstract

For many decades, it was assumed that the characteristics of magnetic domain walls were determined by material properties and the walls were moved by magnetic fields. In the past few years, it has been shown that domain walls behave differently on the nanometer scale. Domain walls in small elements exhibit complex spin arrangements that strongly deviate from the wall types commonly encountered in magnetic thin-film systems, and they can be modified by changing the geometry of the element. Domain walls in nanowires can also be moved by injecting electrical current pulses. Whereas wall propagation is qualitatively explained by a spin transfer from the conduction electrons to the spins of the domain wall, important aspects of the observations cannot be explained by present models. Examples include the observation of a drastic transformation of the wall structure upon current injection and domain wall velocities that tend to be orders of magnitude smaller than anticipated from theory.

Keywords: magnetic properties, nanoscale.

Introduction

The theory of magnetic domains as proposed 100 years ago by Weiss¹ is incomplete if only the domains (i.e., the regions of different magnetization direction) are considered. Equally important are the transition zones between the domains—the domain walls.

Research in domain walls spans many decades. It started with conceptual studies of wall types based on energy considerations and evolved to experimental studies to visualize walls by various methods of increasing sophistication and complexity. Domain walls were also extensively studied indirectly. They determine, to a great extent, the magnetization reversal upon applying a magnetic field. Recently, a new aspect of magnetic domain walls has been attracting attention: domain walls are considered as possible objects for high-speed logic, where each wall represents a single bit.^{2,3} The pioneering prediction^{4,5} and confirmation^{6–18} that domain walls can also be moved by spin-polarized electrical current offers an attractive alternative in designing novel devices such as sensors and magnetic random-access memories.¹⁹

Driven by these enormous prospects for technological applications, active studies of domain walls are underway worldwide. Along the “long and winding road”²⁰ to applications, one encounters interesting

physical phenomena in domain walls in nanoscale elements and nanowires. This article reviews recent progress in the understanding and controlling of domain wall properties in constrained geometries, and in the investigation of spin transfer to move domain walls using current.

Domain Wall Types

The textbook example of a domain wall is the 180° Bloch wall in a uniaxial magnetic material. In the gradual transition from the magnetization direction in one domain to the opposite one in the adjacent domain, the spins rotate in the plane perpendicular to the wall normal and point in directions that are not the energetically preferred, easy-magnetization directions. Therefore, to minimize this anisotropy energy, the domain wall should be kept narrow. Exchange, on the other hand, requires that the angle between adjacent spins be as small as possible, ideally zero, and hence the wall should be wide. The interplay between these two energy contributions leads to a finite domain wall width. This width and the wall profile can be derived analytically using only the two material parameters involved, the exchange constant and the anisotropy energy.

The one-dimensional (1D) Bloch wall rarely exists and is only justified in an in-

finite sample or if anisotropy is very large. In a finite system, dipolar contributions need to be taken into account. In a thin film with in-plane anisotropy, Néel proposed another type of domain wall, with the magnetization rotating entirely within the plane. This Néel wall avoids large stray field energy and hence is favored. In contrast to the Bloch wall, the narrow core region of the Néel wall is accompanied by long tails extending over micrometer distances to locally reduce internal stray fields. Both the Bloch wall and the Néel wall are limiting cases of a more complex wall-type phase diagram with thickness and anisotropy.²¹ Intermediate wall types include, in particular, asymmetric walls of both Bloch and Néel characters.

Lateral confinement leads to even more pronounced geometrical effects. Various types of domain walls arise in micro- and nanostructures because of the demagnetizing energy at the edges. This in turn offers the possibility to finely tune the wall properties, such as the wall width. This is an important aspect, because it enables the use of domain walls as individual tailored objects, and determines, for instance, the resistance or the dynamic properties of the domain wall.

Domain Walls Tailored by Geometry

Bruno was the first to investigate the domain wall width in geometrical constrictions.²² Using a 1D analytical approach, he predicted that Bloch walls shrink in constrictions that are smaller in size than the width of the unconstrained wall. At these scales, the wall width is determined solely by geometry and not the material parameters. In this model, dipolar effects are neglected, and planar Bloch walls are assumed to be pinned at the constriction. However, dipolar contributions are not negligible at the constriction edges, and the wall can also bend, thus resembling a 2D object. Micromagnetic simulations have been used to estimate these effects.^{23,24} Similar to the 1D model,²² the wall width is reduced in constrictions. While the physics is well described by the analytical model, the restriction to 1D makes the model fail to predict the wall width reduction quantitatively. The wall bends outside the constriction area. Furthermore, except for the shortest constrictions, the dipolar energy at the constriction edges forces the magnetization to be parallel to the edges such that the wall becomes Néel rather than Bloch in type, even in cases with large uniaxial anisotropy.

Experimentally, a reduction of the Bloch wall width was observed in nanometer-sized constrictions.²⁵ To systematically as-

assess the geometrical confinement of domain walls, a quantitative study was performed on 180° Néel walls.²⁶ These walls were stabilized in thin $\text{Fe}_{20}\text{Ni}_{80}$ (Permalloy) elements containing a constriction by utilizing a rectangular shape which favors an antiparallel two-domain state. The wall structure in the constriction was measured using high-resolution spin-polarized scanning electron microscopy (spin-SEM, or SEMPA, which stands for SEM with polarization analysis)²⁷ and compared with micromagnetic simulations.

Figure 1a shows such a domain wall centered at a constriction. It attains a complex 2D configuration that is asymmetric. We found that the average width of domain walls can be tuned by the dimensions of the element and the constriction width and length.²⁶ Because of the extended tails of Néel walls, the wall in micrometer-sized elements is confined. Its width thus decreases when the lateral size of the magnetic element decreases. In addition, by tuning the constriction dimensions, the Néel wall width can also be modified continuously (Figure 1b). It is strongly confined in small and narrow constrictions but stretched for wide constrictions, owing to significant dipolar contributions at the constriction edges. Ninety-degree Néel walls in T-shaped junctions exhibit the same behavior: the wall width in the contact region strongly depends on the contact dimensions.²⁸

The prototypical Néel and Bloch walls considered in these studies are not the only wall types encountered in small elements. Thin and long nanowires of low-anisotropy magnetic materials require the magnetization to be aligned along the wire to reduce dipolar energy, leading to walls with the magnetizations in neighboring domains pointing toward each other (“head-to-head”) or away from each other (“tail-to-tail”). Apart from the magnetization direction, head-to-head and tail-to-tail walls are equivalent. The detailed spin configuration of these walls is determined by the dimensions of the wire: thin and narrow wires favor a wall with a transverse magnetization component; thicker and wider wires support a vortex structure. The phase diagram for the occurrence of transverse and vortex walls with wire geometry has been calculated using micromagnetic simulations.^{29,30} Experimentally, the transverse-to-vortex boundary has been identified in Co rings of varying width and thickness.³¹ However, the transition is shifted to larger thicknesses, because the experiment probes the remanent state after the application of a large field rather than the equilibrium state, which extends the stability area of the transverse wall.

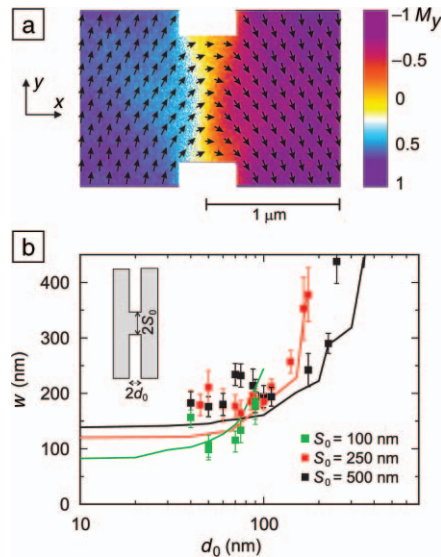


Figure 1. Magnetic domain walls in 7.5-nm-thick $\text{Fe}_{20}\text{Ni}_{80}$ rectangles $10\ \mu\text{m} \times 4\ \mu\text{m}$ in size pinned at a constriction, measured by spin-polarized scanning electron microscopy (spin-SEM). (a) The image shows the center part of the rectangle that defines a two-domain state, with magnetization along $+y$ (left of the constriction) and $-y$ (right of the constriction). The color code represents the magnetization component M_y , and the arrows give the in-plane magnetization direction as determined from the measured M_x and M_y components. The magnetization configuration is asymmetric in appearance, resulting in a wall that is wider toward the top than the bottom constriction (colored yellow for vanishing M_y). The constriction dimensions are $d_0 = 225\ \text{nm}$ and $S_0 = 500\ \text{nm}$, as defined by the inset in (b). (b) Domain wall width w versus constriction dimension d_0 in $\text{Fe}_{20}\text{Ni}_{80}$, with $S_0 = 100\ \text{nm}$ (green), $250\ \text{nm}$ (red), and $500\ \text{nm}$ (black). Squares are experimental values, and lines are micromagnetic simulations. The inset shows the element and defines constriction width d_0 and length S_0 . (Adapted from Reference 26.)

In general, magnetic domain walls in small elements and wires behave as complex (and only rarely as 1D) objects. Experiments demonstrate the ability to control domain wall profiles and dimensions using geometry. For identical material parameters, the domain wall width can be varied over a wide range, and even the wall type can be completely changed. This tunability offers the possibility to finely tailor domain walls by geometry.

Domain Wall Motion

Not only are the static properties of magnetic domain walls important. All current and future applications require precise control of the dynamics of the magnetic state; that is, the temporal evolution of the magnetization matters. Understanding and controlling the dynamics of a domain wall means, on a macroscopic level, understanding and controlling magnetization reversal: domain wall propagation generally is by far the most effective way to reverse magnetization, be it in bulk or a thin film. The standard way to move a domain wall is by applying a magnetic field. Above a certain field, the domain wall starts to propagate. The situation is basically the same for nanowires. Magnetization reversal results from the propagation of a domain wall, with the wall velocity given by the applied magnetic field.³² A scheme for logic based on magnetic domain walls exploits this fact.^{2,3} In the past few years, various studies focused on wall propagation in nanowires, particularly in the low-field regime,^{32,33} on the transition from a steady state to a turbulent regime,^{30,34} and on the importance of edge roughness on wall velocity.^{35,36}

Instead of a magnetic field, an electrical current flowing in the magnetic element can be used to move a domain wall. This was first described by Berger.^{4,5} Several mechanisms of how current acts on domain walls were proposed and discussed. First—and probably most obvious—is the Oersted field, the circumferential magnetic field accompanying current flow in the wire as described by Ampère’s law. Second, the Hall effect within the wall creates a hydromagnetic drag force on the wall.^{4,37,38} Third, the exchange interaction between the $3d$ electrons in the ferromagnet and the spin-polarized conduction electrons results in a torque and a transfer of spin momentum from the drifting electrons to the domain wall.⁵ This latter effect is believed to be the predominant mechanism for moving a wall in a magnetic nanowire, and it is also responsible for current-induced magnetization switching in nanopillars.³⁹ Recently, new theoretical models of spin-transfer torque have been proposed. In particular, the underlying Landau–Lifshitz–Gilbert equation has been extended by additional torque terms,^{40,41} the importance of linear versus angular momentum transfer has been estimated,⁴² and nonadiabatic spin transfer has been proposed.^{43–45}

Experimentally, current-induced domain wall motion was first detected in continuous films.^{6–8} The interpretation of these early experiments was hampered by the fact that in films a domain wall is a two-

dimensional moving front of complex geometry. However, the technical advances in nanoscale patterning helped overcome these difficulties. In nanowires, domain wall type and geometry are better controlled and the current path is well defined. Recent experiments on such wires have convincingly shown that spin torque is able to displace domain walls. One approach detects wall displacement by measuring the signal changes triggered by a passing domain wall, be it with anisotropic¹⁰ or giant⁹ magnetoresistance or with induced Hall voltage.¹⁸ Alternatively, the wall position can be determined before and after current injection using microscopy techniques such as magnetic force microscopy (MFM),^{12,14} the magneto-optical Kerr effect^{13,15} or spin-SEM¹⁷ (Figure 2). In these experiments, a vortex domain wall is introduced in the wire by applying a magnetic field. Then, current pulses are injected into the wire at zero field, and the position of the wall after current injection is determined by magnetic imaging.

After the application of a current pulse of 0.5–10 μs , both head-to-head and tail-to-tail walls move opposite to the direction of the current flow. By reversing the current direction, the walls can be moved back and forth along the wire. This demonstrates that spin transfer is the predominant mechanism for domain wall motion. The Oersted field is weak and would have different ac-

tion on head-to-head and tail-to-tail walls. The hydromagnetic drag force is expected to be negligible at these thicknesses and would move the wall in the opposite direction. Although most of the experiments on current-induced wall motion have so far been performed on Permalloy, it is worth mentioning that the observed effect is much more general. Domain wall motion in the direction of the charge carriers was also reported for the ferromagnetic semiconductor GaMnAs.¹⁵

We note that domain wall motion by current is only observed above a certain (large) threshold current. In Permalloy, for instance, the current density is much larger than what the nanowire can sustain for an extended period of time, typically on the order of 10^{11} – 10^{12} A/m² for single-layer Permalloy.^{13,14,16,17,46,47} The origin of the threshold current is not yet clear and still under debate. Depending on the theoretical model, it is either an intrinsic^{42,48} or an extrinsic^{45,49} characteristic of current-induced domain wall motion. Experimental data relating observed threshold currents to different wall types or wire dimensions are scarce,¹⁶ and no investigation on extrinsic effects such as the influence of pinning sites due to the sample fabrication process has been published. Remarkably, the threshold current density is reduced in spin-valve and multilayer structures,^{9,11} which could be related to the presence of

thick conducting underlayers, and also in GaMnAs wires at low temperature.¹⁵

The fundamental mechanism underlying the spin-torque model is the precession of the spins in the propagating domain wall. Hence, irrespective of the details of the theoretical model, the wall velocity can be expected to depend on the spin-precession frequency. An important parameter to check the models therefore is the domain wall velocity, which can be extracted from a series of images like those in Figure 2. The average wall velocity can be calculated from the distance traveled by the wall divided by the duration of the current pulse. All published data for Permalloy find average (initial) velocities on the order of 1 m/s for current pulse durations in the microsecond range.^{14,17,50} This is much smaller than theoretical predictions, which give domain wall velocities on the order of 100 m/s.^{42,44,45,48}

Note that the velocity discussed in the preceding paragraph is the average wall velocity during the first current injections. As revealed by Figure 2, the distance traveled by the wall fluctuates from injection to injection, with the wall intermittently standing still. It was proposed¹⁴ that the differences in displacement are possibly related to the pinning by randomly located defects. Such variations in the wall velocity were also observed with different samples.^{17,50} Figure 3 presents the evolu-

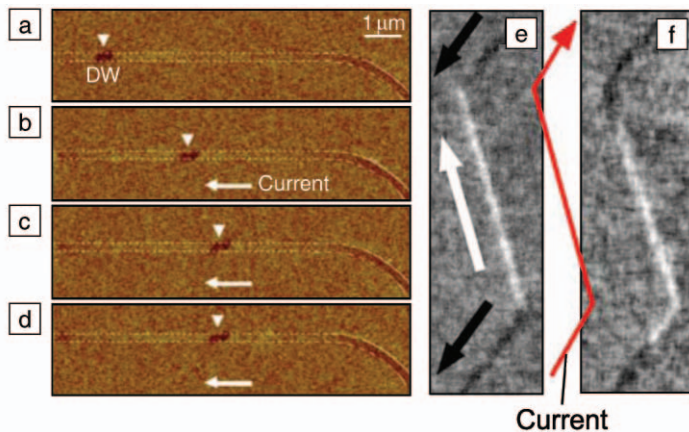


Figure 2. Magnetic images showing the motion of a domain wall (DW) in Permalloy ($\text{Fe}_{20}\text{Ni}_{80}$) upon successive current-pulse injections, for current densities slightly above threshold. (a)–(d) A tail-to-tail wall, imaged by magnetic force microscopy as a dark contrast, is moved to the right, with the current flowing to the left. Current density, 1.2×10^{12} A/m²; pulse duration, 0.5 μs ; wire dimensions, 240 nm \times 10 nm. The scale bar in (a) applies to (b)–(d) also. (Used with permission from Reference 14.) (e)–(f) Head-to-head and tail-to-tail walls imaged by spin-polarized scanning electron microscopy (spin-SEM). Spin-SEM maps directly the magnetization contrast; that is, black and white wires are magnetized along the directions given by the black and white arrows. The walls move from the initial position at the bends shown in (e) to a position in the straight wire shown in (f), after injection of a 10- μs -long current pulse, with the current direction indicated by the red arrow. Current density, 2.2×10^{12} A/m²; wire dimensions, 500 nm \times 10 nm; length of straight wire segment, 20 μm . (From Reference 17.)

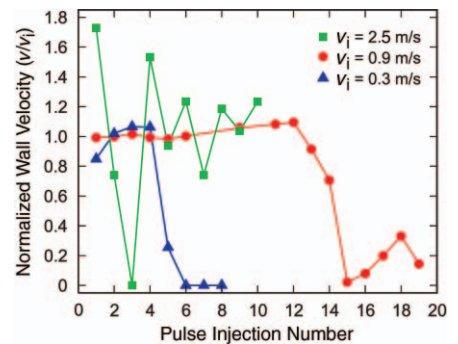


Figure 3. Normalized domain wall velocity as a function of the number of current pulses, as determined from magnetic force microscopy or spin-polarized scanning electron microscopy images for Permalloy wires of different widths and thicknesses. Green squares, 230 nm \times 10 nm;¹⁴ red circles, 300 nm \times 27 nm;⁵⁰ blue triangles, 500 nm \times 10 nm.¹⁷ For ease of comparison, the velocities have been normalized by division with the initial velocity v_i , defined as the mean over the first four injections; these velocities are 2.5 m/s, 0.9 m/s, and 0.3 m/s, respectively.

tion of wall velocity with subsequent injections for Permalloy wires of varying dimensions. It clearly illustrates that current-induced wall motion in general is a stochastic process.

Figure 3 also shows that the vortex wall velocity decays for a constant current density after a few injections to a few tens of injections. Eventually, the wall comes to a complete stop. This is neither caused by material degradation of the sample, as it is possible to reset the system using a magnetic field and reproduce the experiment, nor is it related to strong pinning defects. The walls move back and forth beyond the position of final arrest upon initial injections; moreover, they stop at different positions after each field reset.¹⁷

Using high-resolution imaging of the walls, we discovered that this final stop of the wall is related to a drastic change in the domain wall configuration. Images have been taken after each injection, as shown in Figure 4. After the first injection, the wall is a vortex configuration that corresponds well with the equilibrium configuration calculated by micromagnetic simulations. With subsequent injections, the configura-

tion changes. Although the wall still contains a vortex core, it has acquired a transverse component. Once the wall becomes immobile after additional current injections, the wall structure is changed drastically: the vortex has completely disappeared and a transverse wall has formed. In most instances, this transverse wall is still appreciably distorted. Further current injections of the same amplitude will no longer move the wall. These results demonstrate that the current not only drives wall motion but also induces strong deformations of the 2D wall structure.

Recent theories qualitatively predict some domain wall distortion induced by the spin current. One-dimensional models based on the adiabatic approximation predict a transient distortion of the wall structure, which builds up during the first few nanoseconds.⁵¹ Waintal and Viret⁴³ anticipate significant distortions of the wall structure up to the point at which the wall switches between different types. A step beyond 1D models has been taken with 2D micromagnetic simulations. For a wire narrower than ours, a periodic transformation of the wall structure from vortex to transverse has been found, although at larger current densities.⁴⁵

We have suggested that the wall transformation may be induced by a Lorentz-type force on the vortex core.¹⁷ A very recent model based on adiabatic spin transfer supports this view.⁵² Such a lateral force might move the vortex off-center and expel it at the wire edge.^{45,49,53,54} Our experiments also show that the resulting transverse wall cannot be moved at the same current density as the vortex wall. Recent calculations^{49,53,54} corroborate this finding. In a nonadiabatic approximation including defects, they predict that the threshold current density is larger for a transverse wall than for a vortex wall.

Two-dimensional micromagnetic simulations thus qualitatively explain our observations. Quantitatively, discrepancies still exist regarding the threshold current density, the wall velocity, and the time scales. The transformation from a vortex to a transverse wall is predicted to occur within tens of nanoseconds, while it is observed only after several pulses of microsecond duration.

Conclusions

Some recent progress related to the static properties and the dynamics of domain walls in nanometer-sized constrained geometries has been reviewed. Domain walls are no longer defined by the material properties alone, as their type and profile strongly depend on geometry. Various types of domain walls with different complexity can be stabilized in constrained

systems, and geometry turns out to be an additional versatile parameter to tailor walls. Using lateral constrictions of varying size, the width of a 180° Néel wall can be tuned from a few nanometers to several hundred nanometers.

Controlling the dynamics of the domain wall is also very important, particularly when contemplating domain-wall-based devices. Of particular interest is the ability to move domain walls by having a current flowing through the magnetic domain wall rather than using a magnetic field. Head-to-head domain walls are moved back and forth in thin Permalloy nanowires by applying current pulses above a current threshold. The current induces distortions of the 2D wall structure that can eventually lead to the transformation of a vortex wall into a transverse wall, as observed by high-resolution microscopy. Such a change in spin configuration influences the wall velocity: when transformed into a transverse wall, the wall stops.

Current-induced domain wall motion is based on spin-transfer torque. Models have recently been proposed to describe wall motion. Experimental findings are qualitatively reproduced. Quantitative discrepancies regarding predicted velocities and time scales remain, and several aspects such as the origin of the current threshold, and the effects of roughness and temperature,^{46,55} are still under debate. Controlling domain wall displacement in nanostructures using current pulses is still in its early stages but already presents interesting perspectives. Alternative approaches with ac currents are also being explored.⁵⁶ We are convinced that further experiments and theoretical developments will lead to a much better understanding of spin transfer, so that one day it will become feasible to exploit the interesting prospects of the effect and apply it in novel devices.

References

1. P. Weiss, *J. de Physique* **6** (1907) p. 661.
2. D.A. Allwood, G. Xiong, M.D. Cooke, C.C. Faulkner, D. Atkinson, N. Vernier, and R.P. Cowburn, *Science* **296** (2002) p. 2003.
3. D.A. Allwood, G. Xiong, C.C. Faulkner, D. Atkinson, D. Petit, and R.P. Cowburn, *Science* **309** (2005) p. 1688.
4. L. Berger, *J. Phys. Chem. Solids* **35** (1974) p. 947.
5. L. Berger, *J. Appl. Phys.* **55** (1984) p. 1954.
6. P.P. Freitas and L. Berger, *J. Appl. Phys.* **57** (1985) p. 1266.
7. C.-Y. Hung and L. Berger, *J. Appl. Phys.* **63** (1988) p. 4276.
8. L. Gan, S.H. Chung, K.H. Ashenbach, M. Dreyer, and R.D. Gomez, *IEEE Trans. Magn.* **36** (2000) p. 3047.
9. J. Grollier, D. Lacour, V. Cros, A. Hamzić, A. Vaurès, A. Fert, D. Adam, and G. Faini, *J. Appl. Phys.* **92** (2002) p. 4825.

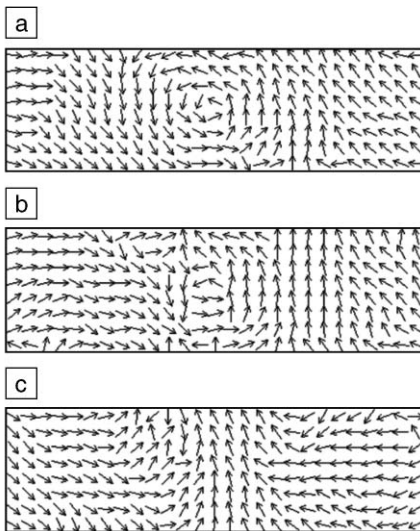


Figure 4. High-resolution experimental images of the spin structure of a domain wall in an Fe₂₀Ni₈₀ wire of 500 nm width and 10 nm thickness after subsequent current injections. The wall transforms from (a) the initial vortex state, to (b) a vortex core with a large transverse component, and, finally, (c) to a transverse wall. This wall no longer moves further with the current density of 2.2×10^{12} A/m². The arrow images are constructed from the two orthogonal in-plane magnetization components taken by spin-SEM. Image size: 1600 nm × 500 nm. (Adapted from Reference 17.)

10. M. Kläui, C.A.F. Vaz, J.A.C. Bland, W. Wernsdorfer, G. Faini, E. Cambril, and L.J. Heyderman, *Appl. Phys. Lett.* **83** (2003) p. 105.
11. J. Grollier, P. Boulenc, V. Cros, A. Hamzić, A. Vaurès, A. Fert, and G. Faini, *Appl. Phys. Lett.* **83** (2003) p. 509.
12. M. Tsoi, R.E. Fontana, and S.S.P. Parkin, *Appl. Phys. Lett.* **83** (2003) p. 2617.
13. N. Vernier, D.A. Allwood, D. Atkinson, M.D. Cooke, and R.P. Cowburn, *Europhys. Lett.* **65** (2004) p. 526.
14. A. Yamaguchi, T. Ono, S. Nasu, K. Miyake, K. Mibu, and T. Shinjo, *Phys. Rev. Lett.* **92** 077205 (2004).
15. M. Yamanouchi, D. Chiba, F. Matsukura, and H. Ohno, *Nature* **428** (2004) p. 539.
16. M. Kläui, C.A.F. Vaz, J.A.C. Bland, W. Wernsdorfer, G. Faini, E. Cambril, L.J. Heyderman, F. Nolting, and U. Rüdiger, *Phys. Rev. Lett.* **94** 106601 (2005).
17. M. Kläui, P.-O. Jubert, R. Allenspach, A. Bischof, J.A.C. Bland, G. Faini, U. Rüdiger, C.A.F. Vaz, L. Vila, and C. Vouille, *Phys. Rev. Lett.* **95** 026601 (2005).
18. D. Ravelosona, D. Lacour, J.A. Katine, B.D. Terris, and C. Chappert, *Phys. Rev. Lett.* **95** 117203 (2005).
19. S.S.P. Parkin, "Shiftable magnetic shift register and method of using the same," U.S. Patent 6,834,005 (December 21, 2004).
20. P. McCartney, "The Long and Winding Road," by J. Lennon and P. McCartney, *Let it Be* (Apple Records/EMI Music, 1970).
21. K. Ramstöck, W. Hartung, and A. Hubert, *Phys. Status Solidi A* **155** (1996) p. 505.
22. P. Bruno, *Phys. Rev. Lett.* **83** (1999) p. 2425.
23. P.-O. Jubert and R. Allenspach, *J. Magn. Magn. Mater.* **290–291** (2005) p. 758.
24. V.A. Molyneux, V.V. Osipov, and E.V. Ponizovskaya, *Phys. Rev. B* **65** 184425 (2002).
25. O. Pietzsch, A. Kubetzka, M. Bode, and R. Wiesendanger, *Phys. Rev. Lett.* **84** (2000) p. 5212.
26. P.-O. Jubert, R. Allenspach, and A. Bischof, *Phys. Rev. B* **69** 220410(R) (2004).
27. R. Allenspach, *J. Magn. Magn. Mater.* **129** (1994) p. 160.
28. T. Haug, C.H. Back, J. Raabe, S. Heun, and A. Locatelli, *Appl. Phys. Lett.* **86** 152503 (2005).
29. R.D. McMichael and M.J. Donahue, *IEEE Trans. Magn.* **33** (1997) p. 4167.
30. Y. Nakatani, A. Thiaville, and J. Miltat, *J. Magn. Magn. Mater.* **290–291** (2005) p. 750.
31. M. Kläui, C.A.F. Vaz, J.A.C. Bland, L.J. Heyderman, F. Nolting, A. Pavlovskaya, E. Bauer, S. Cherifi, S. Heun, and A. Locatelli, *Appl. Phys. Lett.* **85** (2004) p. 5637.
32. T. Ono, H. Miyajima, K. Shigeto, K. Mibu, N. Hosoito, and T. Shinjo, *Science* **284** (1999) p. 468.
33. D. Atkinson, D.A. Allwood, G. Xiong, M.D. Cooke, C.C. Faulkner, and R.P. Cowburn, *Nature Mater.* **2** (2003) p. 85.
34. G.S. Beach, C. Nistor, C. Knutson, M. Tsoi, and J.L. Erskine, *Nature Mater.* **4** (2005) p. 741.
35. Y. Nakatani, A. Thiaville, and J. Miltat, *Nature Mater.* **2** (2003) p. 521.
36. F. Cayssol, D. Ravelosona, C. Chappert, J. Ferré, and J.P. Jamet, *Phys. Rev. Lett.* **92** 107202 (2004).
37. W.J. Carr, *J. Appl. Phys.* **45** (1974) p. 394.
38. S.H. Charap, *J. Appl. Phys.* **45** (1974) p. 397.
39. E.B. Myers, D.C. Ralph, J.A. Katine, R.N. Louie, and R.A. Buhrman, *Science* **285** (1999) p. 867.
40. J.C. Slonczewski, *J. Magn. Magn. Mater.* **159** (1996) p. L1.
41. Ya.B. Bazaliy, B.A. Jones, and S.C. Zhang, *Phys. Rev. B* **57** (1998) p. 3213(R).
42. G. Tatara and H. Kohno, *Phys. Rev. Lett.* **92** 086601 (2004).
43. X. Waintal and M. Viret, *Europhys. Lett.* **65** (2004) p. 427.
44. S. Zhang and Z. Li, *Phys. Rev. Lett.* **93** 127204 (2004).
45. A. Thiaville, Y. Nakatani, J. Miltat, and Y. Suzuki, *Europhys. Lett.* **69** (2005) p. 990.
46. A. Yamaguchi, S. Nasu, H. Tanigawa, T. Ono, K. Miyake, K. Mibu, and T. Shinjo, *Appl. Phys. Lett.* **86** 012511 (2005).
47. A. Himeno, S. Kasai, and T. Ono, *Appl. Phys. Lett.* **87** 243108 (2005).
48. A. Thiaville, Y. Nakatani, J. Miltat, and N. Vernier, *J. Appl. Phys.* **95** (2004) p. 7049.
49. J. He, Z. Li, and S. Zhang, *J. Appl. Phys.* **99** 08G509 (2006).
50. P.-O. Jubert, M. Kläui, A. Bischof, U. Rüdiger, and R. Allenspach, *J. Appl. Phys.* **99** 08G523 (2006).
51. Z. Li and S. Zhang, *Phys. Rev. B* **70** 024417 (2004).
52. J. Shibata, Y. Nakatani, G. Tatara, H. Kohno, and Y. Otani, *Phys. Rev. B* **73** 020403 (2006).
53. Y. Nakatani, private communication.
54. L. Thomas, private communication.
55. G. Tatara, N. Vernier, and J. Ferré, *Appl. Phys. Lett.* **86** 252509 (2005).
56. E. Saitoh, H. Miyajima, T. Yamaoka, and G. Tatara, *Nature* **432** (2004) p. 203. □


Advertisers in This Issue

	Page No.
Bruker AXS, Inc.	362
Global School for Advanced Studies	367
High Voltage Engineering	Inside front cover
Huntington Mechanical Labs, Inc.	Outside back cover
Hysitron, Inc.	409
Janis Research Company, Inc.	399
Kurt J. Lesker Company	Inside back cover
MMR Technologies, Inc.	368
National Electrostatics Corp.	408
Penguin Group (USA)	383
Shiva Technologies, Inc.	371
ULVAC Technologies, Inc.	365
Veeco Instruments Inc.	361

For free information about the products and services offered in this issue, check http://www.mrs.org/bulletin_ads

JANIS

CRYOCOOLERS FROM JANIS



- Pulse tube refrigerators
- Gifford-McMahon refrigerators
- Temperatures from 3.5 K – 800 K

Janis Research Company
 2 Jewel Drive Wilmington, MA 01887 USA
 TEL +1 978 657-8750 FAX +1 978 658-0349 sales@janis.com
 Visit our website at www.janis.com

For more information, see http://www.mrs.org/bulletin_ads